

CHAIN WIELDING STRATEGIES FOR MARKOV-CHAIN MONTE CARLO ESTIMATORS IN INCLUSIVE VARIATIONAL INFERENCE

Anonymous authors

Paper under double-blind review

ABSTRACT

Markovian score climbing (MSC) is a recently proposed variational inference (VI) method based on Markov-chain Monte Carlo (MCMC) for minimizing the inclusive Kullback-Leibler (KL) divergence. This paper shows that independent Metropolis-Hastings (IMH) type kernels can automatically trade off bias and variance when used for MSC. In addition, we also show that the variance of the conditional importance sampling kernel, which was originally proposed for MSC, may increase with an additional computational budget. To fix this, we propose to use parallel IMH (PIMH) chains for obtaining stochastic gradients. We find that MSC with PIMH achieves better performance compared to inclusive as well as exclusive VI methods.

1 INTRODUCTION

Given an observed data \mathbf{x} and a latent variable \mathbf{z} , Bayesian inference aims to analyze $p(\mathbf{z}|\mathbf{x})$ given an unnormalized joint density $p(\mathbf{z}, \mathbf{x})$ where the relationship is given by Bayes’ rule such that $p(\mathbf{z}|\mathbf{x}) = p(\mathbf{z}, \mathbf{x})/p(\mathbf{x}) \propto p(\mathbf{z}, \mathbf{x})$. Instead of working directly with the target distribution $p(\mathbf{z}|\mathbf{x})$, variational inference (VI, Jordan et al. 1999; Blei et al. 2017; Zhang et al. 2019) searches for a variational approximation $q_\lambda(\mathbf{z})$ that is similar to $p(\mathbf{z}|\mathbf{x})$ according to a discrepancy measure $D(p, q_\lambda)$.

Naturally, choosing a good discrepancy measure, or objective function, is a critical part of the problem. This fact had lead to a quest for good divergence measures (Li & Turner, 2016; Deng et al., 2017; Wang et al., 2018; Ruiz & Titsias, 2019). So far, the exclusive KL divergence $D_{\text{KL}}(q_\lambda \parallel p)$ (or reverse KL divergence) has been used “exclusively” among various discrepancy measures. This is partly because the exclusive KL is defined as an average over $q_\lambda(\mathbf{z})$, which can be estimated efficiently. By contrast, the inclusive KL is defined as

$$D_{\text{KL}}(p \parallel q_\lambda) = \int p(\mathbf{z}|\mathbf{x}) \log \frac{p(\mathbf{z}|\mathbf{x})}{q_\lambda(\mathbf{z})} d\mathbf{z} = \mathbb{E}_{p(\mathbf{z}|\mathbf{x})} \left[\log \frac{p(\mathbf{z}|\mathbf{x})}{q_\lambda(\mathbf{z})} \right] \quad (1)$$

where the average is taken over $p(\mathbf{z}|\mathbf{x})$. Interestingly, this is a chicken-and-egg problem as our goal is to obtain $p(\mathbf{z}|\mathbf{x})$ in the first place. Despite this challenge, minimizing (1) has drawn the attention of researchers because it can overcome some known limitations of the exclusive KL (Minka, 2005; MacKay, 2001).

For performing inclusive VI, Naesseth et al. (2020); Ou & Song (2020) recently proposed *Markovian score climbing* (MSC), which is a blend of Markov-chain Monte Carlo (MCMC) and variational inference. In MSC, stochastic gradients of the inclusive KL are obtained by operating a Markov-chain in parallel with the VI optimizer. In this paper, we find an interesting property of MSC when it is combined with specific types of MCMC kernels. Specifically, we show that *independent Metropolis-Hastings* (IMH, Robert & Casella 2004) type kernels can automatically trade off bias and variance when used for MSC. This family of kernels includes the *conditional importance sampling* (CIS, Naesseth et al. 2020) kernel, which was originally proposed for MSC. Surprisingly, this automatic tradeoff property is unique to IMH type kernels and does not occur in MCMC kernels with state-dependent proposals such as Hamiltonian Monte Carlo (HMC, Duane et al. 1987; Neal 2011a; Betancourt 2017).

Following our analysis of the CIS kernel, we also show that its performance can degrade with the number of proposals (which is equivalent to the *per-transition computational budget*) used in each Markov-chain transition. As a simple solution to this, we propose to use parallel IMH (MSC-PIMH) chains, which reduce variance given the same amount of computation. We evaluate the performance of MSC with PIMH against other inclusive VI (Bornschein & Bengio, 2015; Naesseth et al., 2020) and exclusive VI (Ranganath et al., 2014; Kucukelbir et al., 2017) methods.

Contribution Summary (i) We show that IMH type kernels (which include the CIS kernel originally used in MSC; ??) automatically perform bias-variance tradeoff(?). (ii) We show that increasing the computation budget of the CIS kernel may *increase* its variance. To overcome this limitation, we propose to use parallel IMH (PIMH) (?). (iii) We evaluate the performance of MSC with PIMH against other inclusive and exclusive VI methods (**Section 4**).

2 BACKGROUND

2.1 INCLUSIVE VARIATIONAL INFERENCE UNTIL NOW

Different inclusive variational A typical way to perform VI is to use stochastic gradient descent (SGD, Robbins & Monro 1951; Bottou 1999), which requires unbiased gradient estimates of the optimization target. In the case of inclusive variational inference, this corresponds to estimating

$$\nabla_{\lambda} D_{\text{KL}}(p \parallel q_{\lambda}) = \mathbb{E}_{p(\mathbf{z}|\mathbf{x})} [-\nabla_{\lambda} \log q_{\lambda}(\mathbf{z})] = -\mathbb{E}_{p(\mathbf{z}|\mathbf{x})} [s(\mathbf{z}; \lambda)] \approx g(\lambda) \quad (2)$$

with some estimator $g(\lambda)$ where $s(\mathbf{z}; \lambda) = \nabla_{\lambda} \log q_{\lambda}(\mathbf{z})$ is known as the *score function*. Evidently, estimating $\nabla_{\lambda} D_{\text{KL}}(p \parallel q_{\lambda})$ requires integrating the score function over $p(\mathbf{z} | \mathbf{x})$, which is prohibitive. Different inclusive variational inference methods form a different estimator g .

Importance Sampling When it is easy to sample from the variational approximation $q_{\lambda}(\mathbf{z})$, one can use importance sampling (IS, Robert & Casella 2004; Owen 2013) for estimating g since

$$\mathbb{E}_{p(\mathbf{z}|\mathbf{x})} [s(\mathbf{z}; \lambda)] \propto \mathbb{E}_{q_{\lambda}} [w(\mathbf{z}) s(\mathbf{z}; \lambda)] \approx \frac{1}{N} \sum_{i=1}^N w(\mathbf{z}^{(i)}) s(\mathbf{z}^{(i)}; \lambda) = g_{\text{IS}}(\lambda) \quad (3)$$

where $w(\mathbf{z}) = p(\mathbf{z}, \mathbf{x})/q_{\lambda}(\mathbf{z})$ is known as the *importance weight*, and $\mathbf{z}^{(1)}, \dots, \mathbf{z}^{(N)}$ are N independent samples from $q_{\lambda}(\mathbf{z})$. This scheme is equivalent to adaptive IS methods (Cappé et al., 2008; Bugallo et al., 2017) since the IS proposal $q_{\lambda}(\mathbf{z})$ is iteratively optimized based on the current samples. Though IS is unbiased, it is highly unstable in practice. A more stable alternative is to use the *normalized weight* $\tilde{w}^{(i)} = w(\mathbf{z}^{(i)})/\sum_{i=1}^N w(\mathbf{z}^{(i)})$, which is known as the self-normalized IS (SNIS) approximation. Unfortunately, SNIS still fails to converge even on moderate dimensional objectives and unlike IS, it is no longer unbiased (Robert & Casella, 2004; Owen, 2013).

3 CHAIN WIELDING STRATEGIES FOR MARKOV-CHAIN MONTE CARLO ESTIMATORS IN INCLUSIVE VARIATIONAL INFERENCE

3.1 OVERVIEW OF PREVIOUS ESTIMATION STRATEGIES

Overview Recently, Naesseth et al. and Ou & Song proposed two similar but independent methods for performing inclusive variational inference. Both methods estimate the score gradient by operating a Markov-chain in parallel with the VI optimization sequence. Also, they both use MCMC kernels that can effectively used the variational approximation $q_{\lambda_t}(\mathbf{z})$. Because of this, compared to previous VI approaches (Ruiz & Titsias, 2019; Hoffman, 2017) that use expensive MCMC kernels such as Hamiltonian Monte Carlo, both methods are computationally efficient.

Markovian Score Climbing and the Single State Estimator In Markovian score climbing (MSC), (Naesseth et al., 2020) estimate the score gradient by performing an MCMC iteration and update the parameters such that

$$\mathbf{z}_t \sim K(\mathbf{z}_{t-1}, \cdot) \quad g_{\text{single-CIS}}(\lambda) = s(\mathbf{z}_t; \lambda) \quad (4)$$

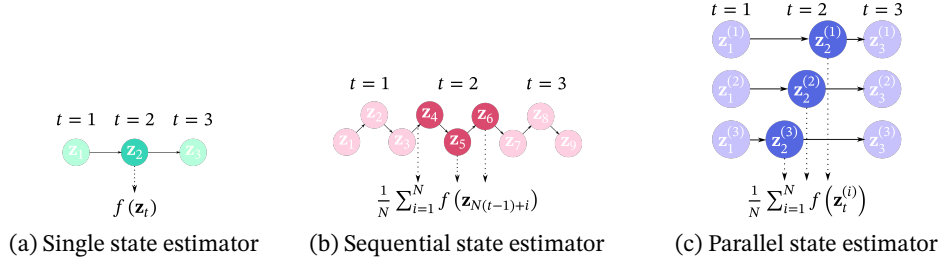


Figure 1: Visualization of different ways of combining MCMC with stochastic approximation variational inference. The index t denotes the stochastic approximation iteration. The dark circles denote the MCMC samples used for estimating the score gradient at $t = 2$.

where $K(\mathbf{z}_{t-1}, \cdot)$ is a MCMC kernel leaving $p(\mathbf{z} | \mathbf{x})$ invariant and $g_{\text{single}}(\boldsymbol{\lambda})$ denotes the score estimator. For $K(\mathbf{z}_{t-1}, \cdot)$, they propose a new type of kernel inspired by particle MCMC Andrieu et al. (2010), the conditional importance sampling (CIS) kernel. Since the estimator uses a *single state* created by the CIS kernel, we call it the single state estimator with the CIS kernel (single-CIS). The CIS kernel internally uses N samples from the $q_{\boldsymbol{\lambda}}(\mathbf{z})$. Thus, when compared to MCMC kernels that only use a single sample from $q_{\boldsymbol{\lambda}}(\mathbf{z})$, it is N times more expensive, but hopefully, statistically superior. Unfortunately, we will show that this is not the case.

Joint Stochastic Approximation and the Sequential State Estimator On the other hand, at each SGD iteration t , (Ou & Song, 2020) perform N sequential Markov-chain transitions and use the average of the intermediate states for estimation. That is, for the index $i \in \{1, \dots, N\}$,

$$\mathbf{z}_{T+i} \sim K^i(\mathbf{z}_T, \cdot) \quad g_{\text{seq-IMH}}(\boldsymbol{\lambda}) = \frac{1}{N} \sum_{i=1}^N s(\mathbf{z}_{T+i}; \boldsymbol{\lambda}) \quad (5)$$

where \mathbf{z}_T is the last Markov-chain state of the previous SGD iteration. For the MCMC kernel, they use the classic independent Metropolis-Hastings (IMH, Robert & Casella 2004, Algorithm 25 Hastings 1970) algorithm, which uses only a single sample from $q_{\boldsymbol{\lambda}}(\mathbf{z})$. Therefore, the cost of N state transitions with IMH is similar to the cost of a single transition with CIS. Since the estimator uses sequential states, we call it the sequential state estimator with the IMH kernel (seq-IMH).

Additional Notes on JSA Before preceeding, we acknowledge that the setup of Ou & Song (2020) is slightly different than what we described. Their MCMC kernel leave $p(\mathbf{z}_j | \mathbf{x}_j)$ invariant for a single datapoint \mathbf{x}_j , which is only possible when the datapoints are independently, identically distributed (*iid*) under the probabilistic model. We interpret their method more generally and assume that we only have a kernel that can leave $p(\mathbf{z} | \mathbf{x})$ invariant.

3.2 OVERVIEW OF MARKOV-CHAIN MONTE CARLO SCORE ESTIMATION STRATEGIES

Single State and Sequential State Estimators The two different MCMC estimators used in MSC and JSA represent two different ways of using a fixed computational budget. The former uses a computationally expensive, but hopefully statistically superior, MCMC kernel with less samples, while the latter uses a cheaper MCMC kernel with more samples. Illustrations of the two schemes are shown in Figures 1a and 1b. Detailed pseudocodes of the considered schemes are provided in the *supplementary material*.

Parallel State Estimator In this work, we will add a new scheme into the mix: the parallel state estimator. Similarly with the sequential state estimator, we use the cheaper IMH kernel, but instead of applying the MCMC kernel N times to a single chain, we apply the MCMC kernel a single time to N parallel Markov-chains. That is, for each Markov-chain $i \in \{1, \dots, N\}$,

$$\mathbf{z}_t^{(i)} \sim K(\mathbf{z}_{t-1}^{(i)}, \cdot) \quad g_{\text{par-IMH}}(\boldsymbol{\lambda}) = \frac{1}{N} \sum_{i=1}^N s(\mathbf{z}_t^{(i)}; \boldsymbol{\lambda}) \quad (6)$$

where $\mathbf{z}_{t-1}^{(i)}$ is the state of the i th chain at the previous SGD step. Computationally speaking, we are still applying $K(\mathbf{z}_{t-1}^{(i)})$ N times in total, so the cost is similar to the sequential state estimator. However, the Markov-chain are N times shorter, which, in a traditional MCMC view, might

Table 1: Computational Cost of Markov-chain Schemes

| | Estimation | | | Stochastic gradient | |
|-------------------------------------|--|------------------------------------|--------------------------------------|--|------------------------------------|
| | $p(\mathbf{z}, \mathbf{x})$ # Eval. | $q_\lambda(\mathbf{z})$ # Eval. | $q_\lambda(\mathbf{z})$ # Samples | $p(\mathbf{z}, \mathbf{x})$ # Grad. | $q_\lambda(\mathbf{z})$ # Grad. |
| ADVI | 0 | 0 | N | N | 0 |
| Single state estimator with CIS | $N - 1$ | N | $N - 1$ | 0 | 1^1 or N^2 |
| Sequential state estimator with IMH | N | N | N | 0 | N |
| Parallel state estimator with IMH | N | N | N | 0 | N |

* N is the number of samples used in each method.

¹ Vanilla CIS kernel.

² Rao-Blackwellized CIS kernel.

seem to result in worse statistical performance. An illustration of the parallel state estimator is shown in Figure 1c

Computational Cost The three scheme using the CIS kernel and the IMH kernel can have different computational cost depending on the parameter N . The computational costs of each scemes are organized in Table 1. In the CIS kernel, N controls the number of internal proposals sampled from $q_\lambda(\mathbf{z})$. In the sequential and parallel state estimators, the IMH kernel only uses a single sample from $q_\lambda(\mathbf{z})$, but applies the kernel N times. When estimating the score, the single state estimator computes $\nabla_\lambda q_\lambda(\mathbf{z})$ only once, while for the sequential and parallel state estimators compute it N times. However, Naesseth et al. (2020) also discuss a Rao-Blackwellized version of the CIS kernel, which also computes the gradient N times.

3.3 THEORETICAL ANALYSIS

Boundedness Assumption Since we derive our bounds on the bias from the total-variation distance, our results assume that the score function is bounded. That is, $\|\nabla_\lambda \log q_\lambda(\mathbf{z})\| < L$ for any λ . This boundedness assumption is reasonable since theoretical guarentees of SGD often assume Lipschitz-continuity of the gradients, from which boundedness follow as a consequence.

Analysis of Bias First, we provide the following bounds on the bias.

Theorem 1. Assuming $w^* = \sup_{\mathbf{z}} p(\mathbf{z}|\mathbf{x})/q_\lambda(\mathbf{z}) < \infty$ for $\forall \lambda$ and the score function is bounded such that $|s(\mathbf{z}; \lambda)| \leq \frac{L}{2}$, the bias of the sequential state estimator with an IMH kernel at iteration t is bounded as

$$\text{Bias}[g_{\text{seq}, t}] \leq L C^{Nt} \quad \text{where} \quad C = \left(1 - \frac{1}{w^*}\right) < 1.$$

Proof. The proof is in the supplementary material.

Theorem 2. Assuming $w^* = \sup_{\mathbf{z}} p(\mathbf{z}|\mathbf{x})/q_{\lambda_t}(\mathbf{z}) < \infty$ for $\forall \lambda$ and that the score function is bounded as $|s(\mathbf{z}; \lambda)| \leq \frac{L}{2}$, the bias of the parallel state estimator with an IMH kernel at iteration t is bounded as

$$\text{Bias}[g_{\text{par}, t}] \leq L C^t \quad \text{where} \quad C = 1 - \frac{1}{w^*} < 1.$$

Proof. The proof is in the supplementary material.

For the sequential mode estimator, Our results suggest that the bias of decreases geometrically with both the number of states N and the SGD iteration t , while for the parallel state estimator, it only decreases with N . Therefore, one might suggest that increasing N will result in a significant reduction in bias compared to the parallel state estimator. However, the geometric rate constant C depends on w^* , which will be exponentially large when the KL divergence is large.

Proposition 1. $w^* = \sup_{\mathbf{z}} p(\mathbf{z}|\mathbf{x})/q_{\lambda}(\mathbf{z})$ is bounded below exponentially by the KL divergence such that $\exp(D_{\text{KL}}(p(\cdot|\mathbf{x}) \parallel q_{\lambda}(\cdot))) \leq w^*$.

Proof. $D_{\text{KL}}(p(\cdot|\mathbf{x}) \parallel q_{\lambda}(\cdot)) = \int p(\mathbf{z}|\mathbf{x}) \log \frac{p(\mathbf{z}|\mathbf{x})}{q_{\lambda}(\mathbf{z})} d\mathbf{z} \leq \int p(\mathbf{z}|\mathbf{x}) \log M d\mathbf{z} = \log w^*$ \square

Therefore, in the initial iterations of VI when the KL divergence has yet been minimized, the constant C will be close to 1. On the other hand, when C is small, the bias will be small regardless of N and t . Thus, increasing N wouldn't result in significant bias reduction.

Theorem 3. For a CIS kernel with N internal proposals, assuming $w^* = \sup_{\mathbf{z}} p(\mathbf{z}|\mathbf{x})/q_{\lambda}(\mathbf{z}) < \infty$ for $\forall \lambda$, $N > 2$, and that the score function is bounded such that $|s(\mathbf{z}; \lambda)| \leq \frac{L}{2}$, the bias of the single state estimator at iteration t is bounded as

$$\text{Bias}[g_{\text{cis},t}] \leq L C^t \quad \text{where} \quad C = \left(1 - \frac{N}{w^*}\right) < 1.$$

Proof. The proof is in the *supplementary material*.

Theorem 4. The variance of the sequential state estimator is

Proof. The proof is in the *supplementary material*.

Theorem 5. The variance of the single mode estimator with a CIS kernel $\mathbb{V}_{q_{\lambda}}[g_{\text{single}}]$ is approximately bounded below such that

$$\mathbb{V}_{q_{\lambda}}[g_{\text{single}}] \geq \frac{N^4 Z^4}{(w(\mathbf{z}_{t-1}) + NZ)^4} \mathbb{V}_{q_{\lambda}}[f_{\text{IS}} | \mathbf{z}_{t-1}], \quad (7)$$

where $Z = \mathbb{E}_{q_{\lambda}}[p(\mathbf{z}, \mathbf{x})/q_{\lambda}(\mathbf{z})] = \int p(\mathbf{z}, \mathbf{x}) d\mathbf{z}$ is the normalizing constant.

Proof. The proof is in the *supplementary material*.

4 EVALUATIONS

4.1 EXPERIMENTAL SETUP

Implementation We implemented MSC with PIMH on top of the Turing (Ge et al., 2018) probabilistic programming framework. Our implementation works with any model described in Turing, which automatically handles distributions with constrained support (Kucukelbir et al., 2017). We use the ADAM optimizer by Kingma & Ba (2015) with a learning rate of 0.01 in all of the experiments. We set the computational budget $N = 10$ and $T = 10^4$ for all experiments unless specified.

Considered Baselines We compare MSC-PIMH with **(i)** MSC using the CIS kernel (MSC-CIS, Naesseth et al. 2020), **(ii)** MSC using the CIS kernel with Rao-Blackwellization (MSC-CISRB, Naesseth et al. 2020), **(iii)** the adaptive IS method using SNIS as introduced in Section 2.1 (SNIS), **(iv)** the reweighted wake-sleep algorithm (RWS, Bornschein & Bengio 2015), and **(v)** evidence lower-bound maximization (ELBO, Ranganath et al. 2014). Specifically, we use automatic differentiation VI (ADVI, Kucukelbir et al. 2017) implemented by Turing.

Reinterpreting RWS The original RWS algorithm assumes that independent samples from $p(\mathbf{z}|\mathbf{x})$ are available, possibly with an additional cost. Since this is not the case in our setting, we reinterpret RWS as alternating between cheap (*sleep update*) and expensive (*wake update*) estimates. We respectively use SNIS and HMC for the sleep and wake updates, and perform the wake update every $K = 5$ steps as originally recommended by Bornschein & Bengio (2015).

4.2 HIERARCHICAL LOGISTIC REGRESSION

Experimental Setup We evaluate MSC-PIMH on logistic regression with the Pima Indians diabetes (**pima**, $\mathbf{z} \in \mathbb{R}^{11}$, Smith et al. 1988), German credit (**german**, $\mathbf{z} \in \mathbb{R}^{27}$), and heart disease (**heart**, $\mathbf{z} \in \mathbb{R}^{16}$, Detrano et al. 1989) datasets obtained from the UCI repository (Dua & Graff, 2017). 10% of the data points were randomly selected in each of the 100 repetitions as test data.

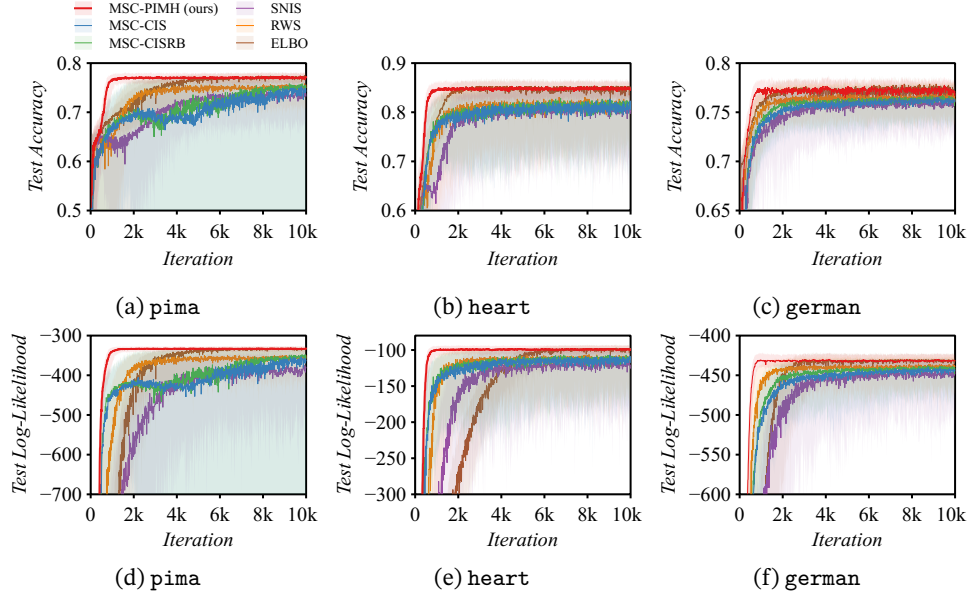


Figure 2: Test accuracy and log-likelihood of logistic regression problems. The solid lines and colored regions are the medians and 80% percentiles computed from 100 repetitions.

Probabilistic Model Instead of the usual single-level probit/logistic regression models used in VI, we choose a more complex hierarchical logistic regression model

$$y_i \sim \text{Bernoulli-Logit}(p), \quad p \sim \mathcal{N}(\mathbf{x}_i^\top \boldsymbol{\beta} + \alpha, \sigma_\alpha^2), \quad \boldsymbol{\beta} \sim \mathcal{N}(\mathbf{0}, \sigma_\beta^2 \mathbf{I}), \quad \sigma_\beta, \sigma_\alpha \sim \mathcal{N}^+(0, 1.0) \quad (8)$$

where $\mathcal{N}^+(\mu, \sigma)$ is a positive constrained normal distribution with mean μ and standard deviation σ , \mathbf{x}_i and y_i are the feature vector and target variable of the i th datapoint. The extra degrees of freedom σ_β and σ_α make this model relatively more challenging.

Results The test accuracy and test log-likelihood results are shown in Figure 2. Our proposed MSC-PIMH is the fastest to converge on all the datasets. Despite having access to high-quality HMC samples, RWS fails to achieve a similar level of performance to MSC-PIMH. However, RWS converges faster than MSC-CIS and MSC-CISRB. Among the two, MSC-CISRB performs only marginally better than MSC-CIS. Meanwhile, SNIS converges the most slowly among inclusive VI methods. Although much slower to converge, ELBO achieves competitive results.

Inclusive VI v.s. Exclusive VI The results of Figure 2 might be misleading to conclude that inclusive and exclusive VI deliver similar results. However, in the parameter space, they choose different optimization paths. This is shown in Figure 3 through the Pareto- \hat{k} diagnostic (Dhaka et al., 2020; Vehtari et al., 2021), which determines how reliable the importance weights are when computed using $q_\lambda(\mathbf{z})$. While the test accuracy suggests that ELBO converges around $t = 2000$, in terms of Pareto- \hat{k} , it takes much longer to converge (about $t = 5000$). This shows that, even if their predictive performance is similar, the inclusive VI chooses paths that have better density coverage as expected.

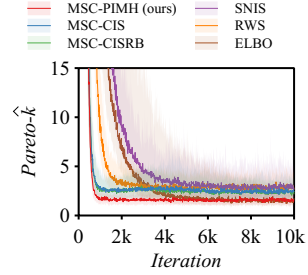


Figure 3: Pareto- \hat{k} statistics result on german. The solid lines and colored regions are the medians and 80% percentiles computed from 100 repetitions.

4.3 MARGINAL LIKELIHOOD ESTIMATION

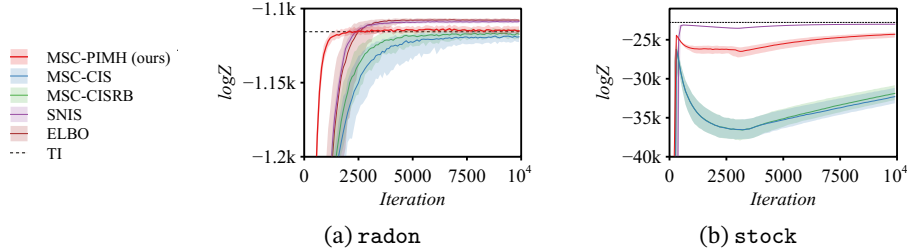


Figure 4: Marginal log-likelihood ($\log Z$) estimates of considered methods. ELBO is omitted in Figure 4b as it failed to deliver reasonable estimates. The solid lines and colored regions are the medians and 80% percentiles computed from 100 repetitions.

Experimental Setup We now estimate the marginal log-likelihood $\log Z$ of a stochastic volatility model (stock, $\mathbf{z} \in \mathbb{R}^{2613}$, Kim et al. 1998) and a hierarchical regression model with partial pooling (radon, $\mathbf{z} \in \mathbb{R}^{175}$, Gelman & Hill 2007) for modeling radon levels in U.S homes. For stock, we use 10 years of the S&P index daily closing price (May 3, 2007, to May 3, 2017). stock is highly challenging as it is both high dimensional and strongly correlated. We estimated the reference marginal likelihood using *thermodynamic integration* (TI, Gelman & Meng 1998; Neal 2001; Lartillot & Philippe 2006) with HMC implemented by Stan (Carpenter et al., 2017; Betancourt, 2017).

Results The results are shown in Figure 4. On radon, MSC-PIMH converges quickly and provides the most accurate estimate. By contrast, MSC-CIS and MSC-CISRB converge much slowly. SNIS and ELBO, on the other hand, overestimate $\log Z$, which can be attributed to the mode-seeking behavior of ELBO and the small sample bias of SNIS. On stock, SNIS is unexpectedly the most accurate. Unfortunately, MSC-PIMH, MSC-CIS, MSC-CISRB all underestimate $\log Z$. Nevertheless, MSC-PIMH provides much better estimates than the latter two. Lastly, we observe that only ELBO fails to converge given the same amount of SGD steps.

5 RELATED WORKS

Inclusive VI with SGD Our method directly builds on top of MSC (Naesseth et al., 2020), which is a method for minimizing the inclusive KL divergence. While many works minimizing the inclusive KL have emerged (Bornschein & Bengio, 2015; Li et al., 2017; Minka, 2001; Ou & Song, 2020; Kim et al., 2021), only a few have been proposed for general VI based on SGD. Notably, Bornschein & Bengio (2015) use SNIS for estimating the stochastic gradients, while Li et al. (2017) use an MCMC kernel to refine samples from $q_\lambda(\mathbf{z})$ to better resemble samples from $p(\mathbf{z} | \mathbf{x})$. Meanwhile, a synonymous method to MSC, *general stochastic approximation* (GSA) by Ou & Song (2020, Algorithm 1) has been proposed concurrently in the context of discrete latent variables. Kim et al. (2021) recently proposed a method that essentially blends GSA/MS with RWS.

Adaptive MCMC As pointed out by Ou & Song (2020), MSC is structurally equivalent to adaptive MCMC methods. Strong resemblance can be found in methods using stochastic approximation for adapting the proposal distribution used inside the MCMC kernel. In particular, Andrieu & Thoms (2008); Garthwaite et al. (2016) discuss the use of stochastic approximation in adaptive MCMC.

Adaptive IMH Among adaptive MCMC methods, those that use independent proposals (Andrieu & Moulines, 2006; Keith et al., 2008; Holden et al., 2009; Giordani & Kohn, 2010) are the most related to our work. Keith et al. (2008) propose to use *cross-entropy minimization* (Barbakh et al., 2009), which is mathematically identical to inclusive VI, for adaptation. Our work, on the other hand, contrasts with previous adaptive IMH algorithms in that we use SGD for adapting $q_\lambda(\mathbf{z})$. This enables VI methods such as ADVI to consider proposals that are much more complex (Kucukelbir et al., 2017).

Ergodicity and Inclusive VI Meanwhile, in the context of MCMC, Mengersen & Tweedie (1996) showed that it is necessary to ensure $\sup_{\mathbf{z}} w(\mathbf{z}) = M < \infty$ (finite weight condition) for an IMH kernel to be geometrically ergodic. While this might seem less relevant for inclusive VI, the bound

$$D_{\text{KL}}(p \parallel q_\lambda) = \int p(\mathbf{z} \mid \mathbf{x}) \log w(\mathbf{z}) d\mathbf{z} \leq \int p(\mathbf{z} \mid \mathbf{x}) \log M d\mathbf{z} = \log M. \quad (9)$$

suggests that it is in fact a sufficient condition for the KL divergence to be finite. This condition can easily be violated as shown by Andrieu & Thoms (2008). To ensure this does not happen, Giordani & Kohn (2010); Holden et al. (2009) use proposal distributions of the form of $w q_0(\mathbf{z}) + (1 - w) q_\lambda(\mathbf{z})$ for some $0 < w < 1$ for their adaptive IMH sampler. Here, q_0 is supposed to be a heavy tailed distribution in the spirit of defensive mixtures (Hesterberg, 1995). A research direction in the interest of both adaptive MCMC and inclusive VI would be to investigate whether such precaution is actually necessary for convergence. If that is the case, it would be beneficial to consider variational families of heavy-tailed distributions as proposed by Domke & Sheldon (2018) for exclusive VI.

6 CONCLUSIONS

In this paper, we investigated the properties of Markovian score climbing (MSC) with independent Metropolis-Hastings (IMH) type Markov-chain Monte Carlo (MCMC) kernels. We proved that IMH type kernels are able to automatically perform bias-variance tradeoff using their accept-reject mechanism. We also analyzed the limitation of the conditional importance sampling (CIS) kernel originally used in MSC. We then proposed parallel IMH (PIMH) as an alternative that enjoys the benefits of CIS without its limitations. Our experiments verify that MSC combined with PIMH performs well on the considered Bayesian inference problems, even compared to exclusive variational inference methods.

ACKNOWLEDGMENTS

This work initially started in the process of understanding the performance of the Markovian score climbing algorithm by Naesseth et al. (2020). We sincerely thank Hongseok Yang for pointing us to a relevant related work by Kim et al. (2021), Guanyang Wang for insightful discussions about the independent Metropolis-Hastings algorithm, Geon Park and Kwanghee Choi for constructive comments that enriched this paper. We also acknowledge the Computer Science Department of Sogang University for providing computational resources.

REFERENCES

- Christophe Andrieu and Éric Moulines. On the ergodicity properties of some adaptive MCMC algorithms. *The Annals of Applied Probability*, 16(3), August 2006.
- Christophe Andrieu and Johannes Thoms. A tutorial on adaptive MCMC. *Statistics and Computing*, 18(4):343–373, December 2008.
- Christophe Andrieu, Arnaud Doucet, and Roman Holenstein. Particle Markov chain Monte Carlo methods. *Journal of the Royal Statistical Society: Series B (Statistical Methodology)*, 72(3):269–342, June 2010.
- Christophe Andrieu, Anthony Lee, and Matti Vihola. Uniform ergodicity of the iterated conditional SMC and geometric ergodicity of particle Gibbs samplers. *Bernoulli*, 24(2), May 2018.
- Haakon Michael Austad. *Parallel Multiple Proposal MCMC Algorithms*. Master thesis, Norwegian University of Science and Technology, June 2007.
- Wesam Ashour Barbakh, Ying Wu, and Colin Fyfe. *Cross Entropy Methods*, volume 249, pp. 151–174. Springer Berlin Heidelberg, Berlin, Heidelberg, 2009.
- Michael Betancourt. A conceptual introduction to Hamiltonian Monte Carlo. *arXiv:1701.02434 [stat]*, January 2017.
- Michael Betancourt. Hierarchical Modeling, November 2020.

- David M. Blei, Alp Kucukelbir, and Jon D. McAuliffe. Variational inference: A review for statisticians. *Journal of the American Statistical Association*, 112(518):859–877, April 2017.
- Jörg Bornschein and Yoshua Bengio. Reweighted wake-sleep. In *Proceedings of the 3rd International Conference on Learning Representation (ICLR)*, San Diego, California, USA, May 2015.
- Léon Bottou. On-line learning and stochastic approximations. In *On-Line Learning in Neural Networks*, pp. 9–42. Cambridge University Press, first edition, January 1999.
- Monica F. Bugallo, Victor Elvira, Luca Martino, David Luengo, Joaquin Miguez, and Petar M. Djuric. Adaptive importance sampling: The past, the present, and the future. *IEEE Signal Processing Magazine*, 34(4):60–79, July 2017.
- Olivier Cappé, Randal Douc, Arnaud Guillin, Jean-Michel Marin, and Christian P. Robert. Adaptive importance sampling in general mixture classes. *Statistics and Computing*, 18(4): 447–459, December 2008.
- Bob Carpenter, Andrew Gelman, Matthew D. Hoffman, Daniel Lee, Ben Goodrich, Michael Betancourt, Marcus Brubaker, Jiqiang Guo, Peter Li, and Allen Riddell. Stan: A probabilistic programming language. *Journal of Statistical Software*, 76(1), 2017.
- Robert Detrano, Andras Janosi, Walter Steinbrunn, Matthias Pfisterer, Johann-Jakob Schmid, Sarbjit Sandhu, Kern H. Guppy, Stella Lee, and Victor Froelicher. International application of a new probability algorithm for the diagnosis of coronary artery disease. *The American Journal of Cardiology*, 64(5):304–310, August 1989.
- Akash Kumar Dhaka, Alejandro Catalina, Michael R Andersen, Måns Magnusson, Jonathan Huggins, and Aki Vehtari. Robust, accurate stochastic optimization for variational inference. In *Advances in Neural Information Processing Systems (NeurIPS)*, volume 33, pp. 10961–10973. Curran Associates, Inc., 2020.
- Adji Bousso Dieng, Dustin Tran, Rajesh Ranganath, John Paisley, and David Blei. Variational inference via χ upper bound minimization. In *Advances in Neural Information Processing Systems (NIPS)*, volume 30, pp. 2729–2738, Long Beach, California, USA, 2017. Curran Associates, Inc.
- Justin Domke and Daniel R Sheldon. Importance weighting and variational inference. In *Advances in Neural Information Processing Systems*, volume 31. Curran Associates, Inc., 2018.
- Dheeru Dua and Casey Graff. UCI machine learning repository. 2017.
- Simon Duane, Anthony D. Kennedy, Brian J. Pendleton, and Duncan Roweth. Hybrid Monte Carlo. *Physics Letters B*, 195(2):216–222, 1987.
- P. H. Garthwaite, Y. Fan, and S. A. Sisson. Adaptive optimal scaling of Metropolis–Hastings algorithms using the Robbins–Monro process. *Communications in Statistics - Theory and Methods*, 45(17):5098–5111, September 2016.
- Hong Ge, Kai Xu, and Zoubin Ghahramani. Turing: A language for flexible probabilistic inference. In *Proceedings of the 21st International Conference on Artificial Intelligence and Statistics (AISTATS)*, volume 84 of *Proceedings of Machine Learning Research*, pp. 1682–1690. ML Research Press, 2018.
- Andrew Gelman and Jennifer Hill. *Data Analysis Using Regression and Multilevel/Hierarchical Models*. Analytical Methods for Social Research. Cambridge University Press, Cambridge; New York, 2007.
- Andrew Gelman and Xiao-Li Meng. Simulating normalizing constants: From importance sampling to bridge sampling to path sampling. *Statistical Science*, 13(2), May 1998.
- Paolo Giordani and Robert Kohn. Adaptive independent Metropolis–Hastings by fast estimation of mixtures of normals. *Journal of Computational and Graphical Statistics*, 19(2):243–259, January 2010.

- W. K. Hastings. Monte Carlo sampling methods using Markov chains and their applications. *Biometrika*, 57(1):97–109, April 1970.
- Tim Hesterberg. Weighted average importance sampling and defensive mixture distributions. *Technometrics*, 37(2):185–194, May 1995.
- Matthew D. Hoffman. Learning deep latent Gaussian models with Markov chain Monte Carlo. In *Proceedings of the 34th International Conference on Machine Learning*, volume 70 of *Proceedings of Machine Learning Research*, pp. 1510–1519. PMLR, August 2017.
- Lars Holden, Ragnar Hauge, and Marit Holden. Adaptive independent Metropolis–Hastings. *The Annals of Applied Probability*, 19(1), February 2009.
- Yu Hang Jiang, Tong Liu, Zhiya Lou, Jeffrey S. Rosenthal, Shanshan Shanguan, Fei Wang, and Zixuan Wu. MCMC confidence intervals and biases. *arXiv:2012.02816 [math, stat]*, June 2021.
- Michael I. Jordan, Zoubin Ghahramani, Tommi S. Jaakkola, and Lawrence K. Saul. An introduction to variational methods for graphical models. *Machine Learning*, 37(2):183–233, 1999.
- Jonathan M. Keith, Dirk P. Kroese, and George Y. Sofronov. Adaptive independence samplers. *Statistics and Computing*, 18(4):409–420, December 2008.
- Hyunsu Kim, Juho Lee, and Hongseok Yang. Adaptive strategy for resetting a non-stationary markov chain during learning via joint stochastic approximation. In *Proceedings of the 3rd Symposium on Advances in Approximate Bayesian, to Appear*, 2021.
- Sangjoon Kim, Neil Shepherd, and Siddhartha Chib. Stochastic Volatility: Likelihood Inference and Comparison with ARCH Models. *Review of Economic Studies*, 65(3):361–393, July 1998.
- Diederik P. Kingma and Jimmy Ba. Adam: A Method for Stochastic Optimization. In *Proceedings of the 3rd International Conference for Learning Representations (ICLR)*, San Diego, California, USA, 2015.
- Alp Kucukelbir, Dustin Tran, Rajesh Ranganath, Andrew Gelman, and David M. Blei. Automatic differentiation variational inference. *Journal of Machine Learning Research*, 18(14): 1–45, 2017.
- Nicolas Lartillot and Hervé Philippe. Computing Bayes factors using thermodynamic integration. *Systematic Biology*, 55(2):195–207, April 2006.
- Yingzhen Li and Richard E Turner. Rényi divergence variational inference. In *Advances in Neural Information Processing Systems (NIPS)*, volume 29. Curran Associates, Inc., 2016.
- Yingzhen Li, Richard E. Turner, and Qiang Liu. Approximate inference with amortised MCMC. *arXiv:1702.08343 [cs, stat]*, May 2017.
- David J.C. MacKay. Local minima, symmetry-breaking, and model pruning in variational free energy minimization. Technical Report, June 2001.
- K. L. Mengersen and R. L. Tweedie. Rates of convergence of the hastings and metropolis algorithms. *The Annals of Statistics*, 24(1):101–121, 1996.
- David D. L. Minh and Do Le (Paul) Minh. Understanding the Hastings Algorithm. *Communications in Statistics - Simulation and Computation*, 44(2):332–349, February 2015.
- Thomas P. Minka. Expectation propagation for approximate bayesian inference. In *Proceedings of the 17th Conference on Uncertainty in Artificial Intelligence (UAI)*, pp. 362–369, San Francisco, CA, USA, 2001. Morgan Kaufmann Publishers Inc.
- Tom Minka. Divergence measures and message passing. Technical Report MSR-TR-2005-173, January 2005.
- Christian Naesseth, Fredrik Lindsten, and David Blei. Markovian score climbing: Variational inference with $KL(p||q)$. In *Advances in Neural Information Processing Systems (NeurIPS)*, volume 33, pp. 15499–15510. Curran Associates, Inc., 2020.

- Radford M. Neal. Annealed importance sampling. *Statistics and Computing*, 11(2):125–139, 2001.
- Radford M Neal. MCMC using Hamiltonian dynamics. In *Handbook of Markov Chain Monte Carlo*, Handbooks of Modern Statistical Methods, pp. 113–162. Chapman and Hall/CRC, first edition, 2011a.
- Radford M. Neal. MCMC Using Ensembles of States for Problems with Fast and Slow Variables such as Gaussian Process Regression. Dept. of Statistics Technical Report 1011, University of Toronto, January 2011b.
- Zhijian Ou and Yunfu Song. Joint stochastic approximation and its application to learning discrete latent variable models. In *Proceedings of the 36th Conference on Uncertainty in Artificial Intelligence (UAI)*, volume 124 of *Proceedings of Machine Learning Research*, pp. 929–938. ML Research Press, August 2020.
- Art B. Owen. *Monte Carlo Theory, Methods and Examples*. 2013.
- P. H. Peskun. Optimum Monte-Carlo sampling using Markov chains. *Biometrika*, 60(3):607–612, 1973.
- Rajesh Ranganath, Sean Gerrish, and David Blei. Black box variational inference. In *Proceedings of the 17th International Conference on Artificial Intelligence and Statistics (AISTATS)*, volume 33 of *Proceedings of Machine Learning Research*, pp. 814–822, Reykjavik, Iceland, April 2014. ML Research Press.
- Herbert Robbins and Sutton Monro. A Stochastic Approximation Method. *The Annals of Mathematical Statistics*, 22(3):400–407, September 1951.
- Christian P. Robert and George Casella. *Monte Carlo Statistical Methods*. Springer Texts in Statistics. Springer New York, New York, NY, 2004.
- Francisco Ruiz and Michalis Titsias. A contrastive divergence for combining variational inference and MCMC. In *Proceedings of the 36th International Conference on Machine Learning (ICML)*, volume 97 of *Proceedings of Machine Learning Research*, pp. 5537–5545. ML Research Press, June 2019.
- Jack W Smith, J. E. Everhart, W. C. Dickson, W. C. Knowler, and R. S. Johannes. Using the ADAP learning algorithm to forecast the onset of diabetes mellitus. In *Proceedings of the Annual Symposium on Computer Application in Medical Care*, pp. 261–265, November 1988.
- Stan Development Team. Stan modeling language users guide and reference manual, version 2.23.0. 2020.
- Aki Vehtari, Daniel Simpson, Andrew Gelman, Yuling Yao, and Jonah Gabry. Pareto smoothed importance sampling. *arXiv:1507.02646 [stat]*, February 2021.
- Dilin Wang, Hao Liu, and Qiang Liu. Variational inference with tail-adaptive f-Divergence. In *Advances in Neural Information Processing Systems (NIPS)*, volume 31. Curran Associates, Inc., 2018.
- Cheng Zhang, Judith Butepage, Hedvig Kjellstrom, and Stephan Mandt. Advances in variational inference. *IEEE Transactions on Pattern Analysis and Machine Intelligence*, 41(8):2008–2026, August 2019.

A RELATIONSHIP BETWEEN SAMPLING METHODS

We organize the sampling methods described in this work in Table 2.

Table 2: Comparison of Sampling Method Designs

| Algorithm | Origin | Proposal | M-H Test | Acceptance Ratio | Multiple Proposals | Reference |
|-----------------------|--------------------|-------------|----------|------------------|--------------------|----------------------|
| RWMH ¹ | MCMC | Dependent | ✓ | M-H | ✗ | Duane et al. (1987) |
| HMC | MCMC | Dependent | ✓ | M-H | ✗ | |
| SNIS | IS | Independent | ✗ | | ✓ | |
| IMH | MCMC | Independent | ✓ | M-H | ✗ | Naesseth et al. 2020 |
| CIS | PMCMC ⁴ | Independent | ✓ | Barker | ✓ | |
| En. MCMC ² | MCMC | Both | ✓ | Barker | ✓ | |
| PMP MCMC ³ | MCMC | Dependent | ✓ | Barker | ✓ | |
| | | | | | | Neal 2011b |
| | | | | | | Austad 2007 |

¹ Random-walk Metropolis-Hastings

² Ensemble MCMC

³ Parallel multiple proposals MCMC

⁴ Particle MCMC

In this paper, we designated kernels that use independent proposals and perform a Metropolis-Hastings (M-H) test as “IMH type” kernels. While the original paper of CIS does not mention it as an IMH type, we have shown in ?? that it is indeed an IMH type kernel that uses Barker’s acceptance ratio and multiple proposals per transition. This, in turn, reveals close connections with ensemble MCMC by Neal (2011b). While parallel multiple proposals MCMC by Austad (2007) also uses Barker’s acceptance ratio and multiple proposals, it only considers dependent proposals, unlike ensemble MCMC. Although in principle, it should work with independent proposals without modification.

B ADDITIONAL EXPERIMENTAL RESULTS

B.1 EXPERIMENTAL ENVIRONMENT

All of our experiments presented in this paper were executed on a server with 20 Intel Xeon E5-2640 CPUs and 64GB RAM. Each of the CPUs has 20 logical threads with 32k L1 cache, 256k L2 cache, and 25MB L3 cache. All of our experiments can be executed within a few days on a system with similar computational capabilities.

B.2 ADDITIONAL RESULTS OF LOGISTIC REGRESSION EXPERIMENTS

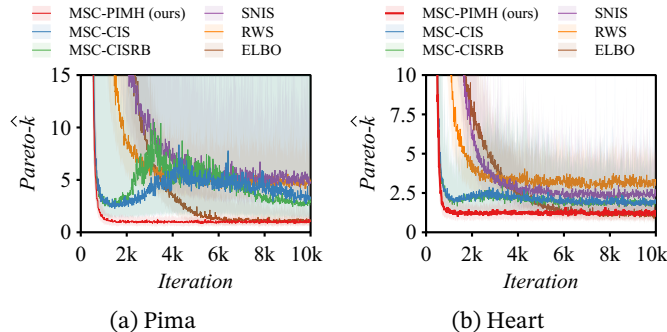


Figure 5: Pareto- \hat{k} results of logistic regression problems. The solid lines are the median of 100 repetitions while the colored regions are the 80% empirical percentiles.

C PSEUDOCODES OF THE CONSIDERED SCHEMES

Algorithm 1: Single State Estimator

Input: MCMC kernel $K(\mathbf{z}, \cdot)$, initial sample \mathbf{z}_0 , initial parameter λ_0 , number of iterations T , stepsize schedule γ_t

for $t = 1, 2, \dots, T$ **do**

- $\mathbf{z}_t \sim K(\mathbf{z}_{t-1}, \cdot)$
- $s(\mathbf{z}; \lambda) = \nabla_{\lambda} \log q_{\lambda}(\mathbf{z})$
- $g_{\text{single}} = s(\mathbf{z}_t; \lambda_{t-1})$
- $\lambda_t = \lambda_{t-1} + \gamma_t g_{\text{single}}$

end

Algorithm 2: Sequential State Estimator

Input: initial sample \mathbf{z}_0 , initial parameter λ_0 , number of iterations T , stepsize schedule γ_t

for $t = 1, 2, \dots, T$ **do**

- $T = N(t - 1)$
- for** $i = 1, 2, \dots, N$ **do**

 - $\mathbf{z}_t \sim K(\mathbf{z}_{T+i}, \cdot)$

- end**
- $s(\mathbf{z}; \lambda) = \nabla_{\lambda} \log q_{\lambda}(\mathbf{z})$
- $g_{\text{seq}} = \frac{1}{N} \sum_{i=1}^N s(\mathbf{z}_{T+i}; \lambda_{t-1})$
- $\lambda_t = \lambda_{t-1} + \gamma_t g_{\text{seq}}$

end

Algorithm 3: Parallel State Estimator

Input: initial samples $\mathbf{z}_0^{(1)}, \dots, \mathbf{z}_0^{(N)}$, initial parameter λ_0 , number of iterations T , stepsize schedule γ_t

for $t = 1, 2, \dots, T$ **do**

- for** $i = 1, 2, \dots, N$ **do**

 - $\mathbf{z}_t^{(i)} \sim K(\mathbf{z}_{t-1}^{(i)}, \cdot)$

- end**
- $s(\mathbf{z}; \lambda) = \nabla_{\lambda} \log q_{\lambda}(\mathbf{z})$
- $g_{\text{par}} = \frac{1}{N} \sum_{i=1}^N s(\mathbf{z}_t^{(i)}; \lambda_{t-1})$
- $\lambda_t = \lambda_{t-1} + \gamma_t g_{\text{par}}$

end

Algorithm 4: Conditional Importance Sampling Kernel

Input: previous sample \mathbf{z}_{t-1} , previous parameter λ_{t-1} , number of proposals N

$\mathbf{z}^{(0)} = \mathbf{z}_{t-1}$

$\mathbf{z}^{(i)} \sim q_{\lambda_{t-1}}(\mathbf{z})$ for $i = 1, 2, \dots, N$

$w(\mathbf{z}^{(i)}) = p(\mathbf{z}^{(i)}, \mathbf{x}) / q_{\lambda_{t-1}}(\mathbf{z}^{(i)})$ for $i = 0, 1, \dots, N$

$\tilde{w}^{(i)} = w(\mathbf{z}^{(i)}) / \sum_{i=0}^N w(\mathbf{z}^{(i)})$ for $i = 0, 1, \dots, N$

$\mathbf{z}_t \sim \text{Multinomial}(\tilde{w}^{(0)}, \tilde{w}^{(1)}, \dots, \tilde{w}^{(N)})$

Algorithm 5: Independent Metropolis-Hastings Kernel

Input: previous sample \mathbf{z}_{t-1} , previous parameter λ_{t-1} ,
 $\mathbf{z}^* \sim q_{\lambda_{t-1}}(\mathbf{z})$
 $w(\mathbf{z}) = p(\mathbf{z}, \mathbf{x})/q_{\lambda_{t-1}}(\mathbf{z})$
 $\alpha = \min(w(\mathbf{z}^*)/w(\mathbf{z}_{t-1}), 1)$
 $u \sim \text{Uniform}(0, 1)$
if $u < \alpha$ **then**
 $\mathbf{z}_t = \mathbf{z}^*$
else
 $\mathbf{z}_t = \mathbf{z}_{t-1}$
end

C.1 ISOTROPIC GAUSSIAN EXPERIMENTS

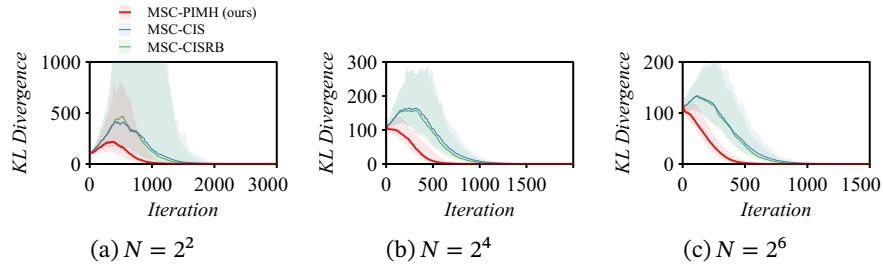


Figure 6: 100-D isotropic Gaussian example with a varying computational budget N . MSC-PIMH converges faster than MSC-CIS and MSC-CISRB regardless of N . Also, the convergence of MSC-PIMH becomes more stable/monotonic as N increases. The solid lines and colored regions are the medians and 80% percentiles computed from 100 repetitions.

We perform experiments with a 100-D isotropic multivariate Gaussian distribution. With Gaussian distributions, convergence can be evaluated exactly since their KL divergence is available in a closed form. We compare the performance of MSC-PIMH, MSC-CIS, and MSC-CISRB with respect to the N (number of proposals for MSC-CIS, MSC-CISRB; number of parallel chains for MSC-PIMH). The results are shown in Figure 6. While MSC-PIMH shows some level of overshoot with $N = 4$, it shows monotonic convergence with larger N . On the other hand, both MSC-CIS and MSC-CISRB overshoots even with $N = 64$. This clearly shows that PIMH enjoys better gradient estimates compared to the CIS kernel.

D NUMERICAL SIMULATION

We present numerical simulations of our analyses in ?? and ?. In particular, we visualize the fact that the variance of the CIS kernel can increase with the number of proposals N when the KL divergence is large, as described in (??).

Experimental Setup We first set the target distribution as $p(\mathbf{z} | \mathbf{x}) = \mathcal{N}(0, 1)$ and the proposal distribution as $q(\mathbf{z}; \mu) = \mathcal{N}(\mu, 2)$ with varying mean. We measure the variance of estimating the score function $s(\mathbf{z}, \mu) = \frac{\partial q(\mathbf{z}; \mu)}{\partial \mu}$ using the CIS, CISRB, and PIMH kernels, given the previous Markov-chain denoted by state \mathbf{z}_{t-1} and computational budget N . For CIS and CISRB, we set a fixed \mathbf{z}_{t-1} , while for PIMH, we randomly sample N samples from $\mathbf{z}_{t-1} \sim p(\mathbf{z} | \mathbf{x})$ (we obtained similar trends regardless of the distribution of \mathbf{z}_{t-1}). The variance is estimated using 2^{14} samples from $K(\mathbf{z}_{t-1}, \cdot)$. We report the variance across varying N and varying KL divergence between $q_\lambda(\mathbf{z})$ and $p(\mathbf{z} | \mathbf{x})$. The latter is performed by varying the difference between the mean of the proposal and the target distributions denoted by $\Delta\mu = \mathbb{E}_{p(\mathbf{z}|\mathbf{x})}[\mathbf{z}] - \mathbb{E}_{q_\lambda}[\mathbf{z}]$.

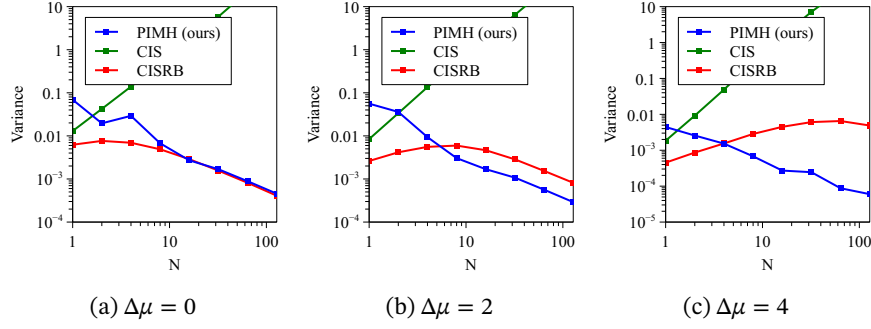


Figure 7: Conditional variance of different MCMC kernels with varying N and varying difference between the mean of the target and proposal distributions.

Results Summary The results are presented in Figure 7. We can see that, when the difference of the mean of the p and q is large, the variance of CISRB *increases* with N . This increasing trend becomes stronger as the KL divergence between p and q increases. While this simulation suggests that CISRB has much smaller variance compared to CIS, our realistic experiments in Section 4 did not reveal such levels of performance gains. It is also visible that PIMH has a slightly larger variance compared to CIS in the small N regime. This is due to the higher acceptance rate of the Metropolis-Hastings acceptance ratio used by PIMH compared to Barker’s acceptance ratio used by CIS (Peskun, 1973; Minh & Minh, 2015).

E PROBABILISTIC MODELS CONSIDERED IN SECTION 4

E.1 HIERARCHICAL LOGISTIC REGRESSION

The hierarchical logistic regression used in Section 4.2 is

$$\begin{aligned}
 \sigma_\beta &\sim \mathcal{N}^+(0, 1.0) \\
 \sigma_\alpha &\sim \mathcal{N}^+(0, 1.0) \\
 \boldsymbol{\beta} &\sim \mathcal{N}(\mathbf{0}, \sigma_\beta^2 \mathbf{I}) \\
 \alpha &\sim \mathcal{N}(0, \sigma_\alpha^2) \\
 p &\sim \mathcal{N}(\mathbf{x}_i^\top \boldsymbol{\beta} + \alpha, \sigma_\alpha^2) \\
 y_i &\sim \text{Bernoulli-Logit}(p)
 \end{aligned}$$

where \mathbf{x}_i and y_i are the predictors and binary target variable of the i th datapoints.

E.2 STOCHASTIC VOLATILITY

The stochastic volatility model used in Section 4.3 is

$$\begin{aligned}
 \mu &\sim \text{Cauchy}(0, 10) \\
 \phi &\sim \text{Uniform}(-1, 1) \\
 \sigma &\sim \text{Cauchy}^+(0, 5) \\
 h_1 &\sim \mathcal{N}\left(0, \frac{\sigma^2}{1 - \phi^2}\right) \\
 h_{t+1} &\sim \mathcal{N}(\mu + \phi(h_t - \mu), \sigma^2) \\
 y_t &\sim \mathcal{N}(0, \exp(h_t))
 \end{aligned}$$

where y_t is the stock price at the t th point in time. We used the reparameterized version where h_t is sampled from a white multivariate Gaussian described by the Stan Development Team (2020).

E.3 RADON HIERARCHICAL REGRESSION

The partially pooled linear regression model used in Section 4.3 is

$$\begin{aligned}
\sigma_{a_1} &\sim \text{Gamma}(\alpha = 1, \beta = 0.02) \\
\sigma_{a_2} &\sim \text{Gamma}(\alpha = 1, \beta = 0.02) \\
\sigma_y &\sim \text{Gamma}(\alpha = 1, \beta = 0.02) \\
\mu_{a_1} &\sim \mathcal{N}(0, 1) \\
\mu_{a_2} &\sim \mathcal{N}(0, 1) \\
a_{1,c} &\sim \mathcal{N}(\mu_{a_1}, \sigma_{a_1}^2) \\
a_{2,c} &\sim \mathcal{N}(\mu_{a_2}, \sigma_{a_2}^2) \\
y_i &\sim \mathcal{N}(a_{1,c_i} + a_{2,c_i} x_i, \sigma_y^2)
\end{aligned}$$

where $a_{1,c}$ is the intercept at the county c , $a_{2,c}$ is the slope at the county c , c_i is the county of the i th datapoint, x_i and y_i are the floor predictor of the measurement and the measured radon level of the i th datapoint, respectively. The model pools the datapoints into their respective counties, which complicates the posterior geometry (Betancourt, 2020).

F PROOFS

Detailed derivation of ??

$$f(\mathbf{z}) = \frac{\sum_{i=0}^N w(\mathbf{z}^{(i)}) f(\mathbf{z}^{(i)})}{\sum_{i=0}^N w(\mathbf{z}^{(i)})} = \frac{\sum_{i=1}^N w(\mathbf{z}^{(i)}) f(\mathbf{z}^{(i)}) + w(\mathbf{z}_{t-1}) f(\mathbf{z}_{t-1})}{\sum_{i=0}^N w(\mathbf{z}^{(i)})} \quad (10)$$

$$= \frac{\sum_{i=1}^N w(\mathbf{z}^{(i)})}{\sum_{i=0}^N w(\mathbf{z}^{(i)})} \frac{\sum_{i=1}^N w(\mathbf{z}^{(i)}) f(\mathbf{z}^{(i)})}{\sum_{i=1}^N w(\mathbf{z}^{(i)})} + \frac{w(\mathbf{z}_{t-1})}{\sum_{i=0}^N w(\mathbf{z}^{(i)})} f(\mathbf{z}_{t-1}) \quad (11)$$

$$= \alpha(\mathbf{z}_{t-1}, \mathbf{z}^{(1:N)}) \frac{\sum_{i=1}^N w(\mathbf{z}^{(i)}) f(\mathbf{z}^{(i)})}{\sum_{i=1}^N w(\mathbf{z}^{(i)})} + r(\mathbf{z}_{t-1} | \mathbf{z}^{(1:N)}) f(\mathbf{z}_{t-1}), \quad (12)$$

where $\alpha(\mathbf{z}_{t-1}, \mathbf{z}^{(1:N)}) = \sum_{i=1}^N w(\mathbf{z}^{(i)}) / \sum_{i=0}^N w(\mathbf{z}^{(i)})$, $f_{IS} = \sum_{i=1}^N w(\mathbf{z}^{(i)}) f(\mathbf{z}^{(i)}) / \sum_{i=1}^N w(\mathbf{z}^{(i)})$, and $r(\mathbf{z}_{t-1} | \mathbf{z}^{(1:N)}) = w(\mathbf{z}_{t-1}) / \sum_{i=0}^N w(\mathbf{z}^{(i)})$.

Taking expectations on both sides, we get

$$\mathbb{E}[f(\mathbf{z})] = \mathbb{E} \left[\alpha(\mathbf{z}_{t-1}, \mathbf{z}^{(1:N)}) \frac{\sum_{i=1}^N w(\mathbf{z}^{(i)}) f(\mathbf{z}^{(i)})}{\sum_{i=1}^N w(\mathbf{z}^{(i)})} \right] + \mathbb{E}[r(\mathbf{z}_{t-1} | \mathbf{z}^{(1:N)}) f(\mathbf{z}_{t-1})] \quad (13)$$

$$= \mathbb{E} \left[\alpha(\mathbf{z}_{t-1}, \mathbf{z}^{(1:N)}) \frac{\sum_{i=1}^N w(\mathbf{z}^{(i)}) f(\mathbf{z}^{(i)})}{\sum_{i=1}^N w(\mathbf{z}^{(i)})} \right] + r(\mathbf{z}_{t-1}) f(\mathbf{z}_{t-1}). \quad (14)$$

Theorem 1. Assuming $w^* = \sup_{\mathbf{z}} p(\mathbf{z}|\mathbf{x})/q_{\lambda}(\mathbf{z}) < \infty$ for $\forall \lambda$ and the score function is bounded such that $|s(\mathbf{z}; \lambda)| \leq \frac{L}{2}$, the bias of the sequential state estimator with an IMH kernel at iteration t is bounded as

$$\text{Bias}[g_{\text{seq}, t}] \leq L C^N t \quad \text{where} \quad C = \left(1 - \frac{1}{w^*}\right) < 1.$$

Proof of Theorem 1. We employ a similar proof strategy with the works of Jiang et al. (2021, Theorem 4).

Let us first denote the empirical distribution of the Markov-chain states at iteration t as

$$\eta_{\text{seq}, t}(\mathbf{z}) = \frac{1}{N} \sum_{i=1}^N K^{N(t-1)+i}(\mathbf{z}_0, \mathbf{z}), \quad (15)$$

and consequently,

$$g_{\text{seq},t}(\boldsymbol{\lambda}) = \int s(\mathbf{z}; \boldsymbol{\lambda}) \eta_{\text{seq},t}(\mathbf{z}) d\mathbf{z}. \quad (16)$$

Now,

$$\left\| \eta_{\text{seq},t}(\cdot) - p(\cdot | \mathbf{x}) \right\|_{\text{TV}} = \left\| \frac{1}{N} \sum_{i=1}^N K^{N(t-1)+i}(\mathbf{z}_0, \cdot) - p(\cdot | \mathbf{x}) \right\|_{\text{TV}} \quad (17)$$

$$\leq \frac{1}{N} \sum_{i=1}^N \left\| K^{N(t-1)+i}(\mathbf{z}_0, \cdot) - p(\cdot | \mathbf{x}) \right\|_{\text{TV}} \quad (\text{Triangle inequality}) \quad (18)$$

For an IMH kernel with $w^* < \infty$, the geometric ergodicity of the IMH kernel (Mengersen & Tweedie, 1996, Theorem 2.1) gives the bound

$$\left\| K^t(\mathbf{z}_0, \cdot) - p(\cdot | \mathbf{x}) \right\|_{\text{TV}} \leq \left(1 - \frac{1}{w^*}\right)^t. \quad (19)$$

But, since in our case w^* is dependent on $\boldsymbol{\lambda}$, our bound is given as

$$\left\| K^t(\mathbf{z}_0, \cdot) - p(\cdot | \mathbf{x}) \right\|_{\text{TV}} \leq \prod_{\tau=1}^t \left(1 - \frac{1}{w^*(\boldsymbol{\lambda}_\tau)}\right). \quad (20)$$

Thus,

$$\left\| \eta_{\text{seq},t}(\cdot) - p(\cdot | \mathbf{x}) \right\|_{\text{TV}} \leq \prod_{\tau=1}^{t-1} \left(1 - \frac{1}{w^*(\boldsymbol{\lambda}_\tau)}\right)^N \frac{1}{N} \sum_{i=1}^N \left(1 - \frac{1}{w^*(\boldsymbol{\lambda}_t)}\right)^i \quad (21)$$

$$\leq \prod_{\tau=1}^{t-1} \left(1 - \frac{1}{w^*}\right)^N \frac{1}{N} \sum_{i=1}^N \left(1 - \frac{1}{w^*}\right)^i \quad (22)$$

$$\leq C^{N(t-1)} \frac{1}{N} \sum_{i=1}^N C^i \quad (23)$$

$$\leq C^{Nt} \quad (24)$$

where $C = 1 - \frac{1}{w^*}$.

Finally, by the definition of the total-variation distance,

$$\text{bias}[g_{\text{seq},t}] \leq \left\| \eta_{\text{seq},t}(\cdot) - p(\cdot | \mathbf{x}) \right\|_{\text{TV}} \quad (25)$$

$$\leq \sup_{h: \mathcal{Z} \rightarrow [-L/2, L/2]} \left| \mathbb{E}_{\eta_{\text{seq},t}(\cdot)}[h] - \mathbb{E}_{p(\cdot | \mathbf{x})}[h] \right| \quad (26)$$

$$= L \left\| \eta_{\text{seq},t}(\cdot) - p(\cdot | \mathbf{x}) \right\|_{\text{TV}} \quad (27)$$

$$\leq L C_1^{Nt}. \quad (28)$$

□

Theorem 2. Assuming $w^* = \sup_{\mathbf{z}} p(\mathbf{z} | \mathbf{x}) / q_{\lambda_\tau}(\mathbf{z}) < \infty$ for $\forall \boldsymbol{\lambda}$ and that the score function is bounded as $|s(\mathbf{z}; \boldsymbol{\lambda})| \leq \frac{L}{2}$, the bias of the parallel state estimator with an IMH kernel at iteration t is bounded as

$$\text{Bias}[g_{\text{par},t}] \leq L C^t \quad \text{where} \quad C = 1 - \frac{1}{w^*} < 1.$$

Proof of Theorem 2. We denote the empirical distribution of the Markov-chain states at iteration t as

$$\eta_{\text{par},t}(\mathbf{z}) = \frac{1}{N} \sum_{i=1}^N K^t(\mathbf{z}_0^{(i)}, \mathbf{z}). \quad (29)$$

and consequently,

$$g_{\text{par},t}(\lambda) = \int s(\mathbf{z}; \lambda) \eta_{\text{par},t}(\mathbf{z}) d\mathbf{z}. \quad (30)$$

Similarly with Theorem 1,

$$\left\| \eta_{\text{par},t}(\mathbf{z}) - p(\cdot | \mathbf{x}) \right\|_{\text{TV}} = \left\| \frac{1}{N} \sum_{i=1}^N K^t(\mathbf{z}_0^{(i)}, \mathbf{z}) - p(\cdot | \mathbf{x}) \right\|_{\text{TV}} \quad (31)$$

$$\leq \frac{1}{N} \sum_{i=1}^N \left\| K^t(\mathbf{z}_0^{(i)}, \cdot) - p(\cdot | \mathbf{x}) \right\|_{\text{TV}} \quad (\text{Triangle inequality}) \quad (32)$$

$$= \left\| K^t(\mathbf{z}_0, \cdot) - p(\cdot | \mathbf{x}) \right\|_{\text{TV}} \quad (\text{Independence}) \quad (33)$$

$$\leq \prod_{\tau=1}^t \left(1 - \frac{1}{w^*(\lambda_\tau)} \right) \quad (34)$$

$$\leq \prod_{\tau=1}^t \left(1 - \frac{1}{w^*} \right) \quad (35)$$

$$\leq C^t \quad (36)$$

where $w^*(\lambda_\tau) = \sup_{\mathbf{z}} p(\mathbf{z}|\mathbf{x})/q_{\lambda_\tau}(\mathbf{z})$ and $C = 1 - 1/w^*$. And, finally the bias is given as

$$\text{bias}[g_{\text{par},t}] \leq L \left\| \eta_{\text{par},t}(\cdot) - p(\cdot | \mathbf{x}) \right\|_{\text{TV}} \quad (37)$$

$$\leq L \sup_{h: \mathcal{Z} \rightarrow [-L/2, L/2]} \left| \mathbb{E}_{\eta_{\text{par},t}(\cdot)}[h] - \mathbb{E}_{p(\cdot|\mathbf{x})}[h] \right| \quad (38)$$

$$= L \left\| \eta_{\text{par},t}(\cdot) - p(\cdot | \mathbf{x}) \right\|_{\text{TV}} \quad (39)$$

$$\leq L C^t. \quad (40)$$

□

Theorem 3. For a CIS kernel with N internal proposals, assuming $w^* = \sup_{\mathbf{z}} p(\mathbf{z}|\mathbf{x})/q_{\lambda}(\mathbf{z}) < \infty$ for $\forall \lambda$, $N > 2$, and that the score function is bounded such that $|s(\mathbf{z}; \lambda)| \leq \frac{L}{2}$, the bias of the single state estimator at iteration t is bounded as

$$\text{Bias}[g_{\text{cis},t}] \leq L C^t \quad \text{where} \quad C = \left(1 - \frac{N}{w^*} \right) < 1.$$

Proof of Theorem 3. Let us first denote the empirical distribution of the Markov-chain states at iteration t as

$$\eta_{\text{cis},t}(\mathbf{z}) = K^t(\mathbf{z}_0, \mathbf{z}), \quad (41)$$

and consequently,

$$g_{\text{cis},t}(\lambda) = \int s(\mathbf{z}; \lambda) \eta_{\text{cis},t}(\mathbf{z}) d\mathbf{z}. \quad (42)$$

The CIS sampler is identical to the iterated sampling importance resampling (i-SIR) algorithm described by Andrieu et al. (2018). They showed that the i-SIR kernel achieves a geometric convergence rate such that

$$\left\| K^t(\mathbf{z}_{t-1}, \cdot) - p(\cdot | \mathbf{x}) \right\|_{\text{TV}} \leq \left(1 - \frac{N-1}{2w^* + N-2} \right)^t. \quad (43)$$

From this, the bound can be shown as

$$\text{bias}[g_{\text{cis},t}] \leq \left\| \eta_{\text{cis},t}(\cdot) - p(\cdot | \mathbf{x}) \right\|_{\text{TV}} \quad (44)$$

$$\leq \sup_{h: \mathcal{Z} \rightarrow [-L/2, L/2]} \left| \mathbb{E}_{\eta_{\text{cis},t}(\cdot)}[h] - \mathbb{E}_{p(\cdot|\mathbf{x})}[h] \right| \quad (45)$$

$$= L \left\| \eta_{\text{cis},t}(\cdot) - p(\cdot | \mathbf{x}) \right\|_{\text{TV}} \quad (46)$$

$$\leq L \left(1 - \frac{N-1}{2w^* + N-2} \right)^t \quad (47)$$

$$\leq L \left(1 - \frac{N}{w^*} \right)^t \quad (48)$$

$$(49)$$

given that $N > 2$. \square

Theorem 4. *The variance of the sequential state estimator is*

Proof of Theorem 4. For notational convenience, let us define $g(\mathbf{z}) = s(\mathbf{z}; \boldsymbol{\lambda})$.

$$\mathbb{V}[g_{\text{seq},t}] \quad (50)$$

$$\geq \mathbb{E}[\mathbb{V}[g_{\text{seq},t} | \mathbf{z}_T]] \quad (51)$$

$$= \mathbb{E} \left[\frac{1}{N^2} \sum_{i=1}^N \mathbb{V}[g(\mathbf{z}_{T+i}) | \mathbf{z}_T] + \frac{2}{N^2} \sum_{i < j} \text{Cov}(g(\mathbf{z}_{T+i}), g(\mathbf{z}_{T+j}) | \mathbf{z}_T) \right] \quad (52)$$

$$= \frac{1}{N^2} \sum_{i=1}^N \mathbb{E}[\mathbb{V}[g(\mathbf{z}_{T+i}) | \mathbf{z}_T]] \quad (53)$$

$$+ \frac{2}{N^2} \sum_{i < j} \mathbb{E}[\text{Cov}(g(\mathbf{z}_{T+i}), g(\mathbf{z}_{T+j}) | \mathbf{z}_T)] \quad (54)$$

$$= \frac{1}{N} \sigma^2 + \frac{2}{N^2} \sum_{i < j} \mathbb{E}_{p(\mathbf{z}_T|\mathbf{x})}[\text{Cov}(g(\mathbf{z}_{T+i}), g(\mathbf{z}_{T+j}) | \mathbf{z}_T)] \quad (\text{Stationarity}) \quad (55)$$

$$= \frac{1}{N} \sigma^2 + \frac{2}{N^2} \sum_{i < j} \mathbb{E}_{p(\mathbf{z}_T|\mathbf{x})}[\text{Cov}(g(\mathbf{z}_{T+i}), g(\mathbf{z}_{T+j}) | \mathbf{z}_T)] \quad (56)$$

\square

Theorem 5. *The variance of the single mode estimator with a CIS kernel $\mathbb{V}_{q_\lambda}[g_{\text{single}}]$ is approximately bounded below such that*

$$\mathbb{V}_{q_\lambda}[g_{\text{single}}] \geq \frac{N^4 Z^4}{(w(\mathbf{z}_{t-1}) + NZ)^4} \mathbb{V}_{q_\lambda}[f_{IS} | \mathbf{z}_{t-1}], \quad (7)$$

where $Z = \mathbb{E}_{q_\lambda}[p(\mathbf{z}, \mathbf{x})/q_\lambda(\mathbf{z})] = \int p(\mathbf{z}, \mathbf{x}) d\mathbf{z}$ is the normalizing constant.

Proof of Theorem 5. By the law of total variance,

$$\mathbb{V}_{q_\lambda}[g_{\text{single}}] \geq \mathbb{V}_{q_\lambda}[g_{\text{single}} | \mathbf{z}_{t-1}]. \quad (57)$$

Write

$$\mathbb{V}_{q_\lambda}[f | \mathbf{z}_{t-1}] = \mathbb{V}_{q_\lambda} \left[\frac{\sum_{i=1}^N w(\mathbf{z}^{(i)})}{\sum_{i=0}^N w(\mathbf{z}^{(i)})} \frac{\sum_{i=1}^N w(\mathbf{z}^{(i)}) f(\mathbf{z}^{(i)})}{\sum_{i=1}^N w(\mathbf{z}^{(i)})} + \frac{w(\mathbf{z}_{t-1})}{\sum_{i=0}^N w(\mathbf{z}^{(i)})} f(\mathbf{z}_{t-1}) \middle| \mathbf{z}_{t-1} \right]. \quad (58)$$

Note that if $a > 0$, then we can approximate the function $\sum_{i=1}^N x_i / (a + \sum_{i=1}^N x_i)$ using the first-order Taylor series expansion about (Z, \dots, Z) by

$$\frac{\sum_{i=1}^N x_i}{a + \sum_{i=1}^N x_i} \approx \frac{NZ}{a + NZ} + \sum_{i=1}^N \frac{a}{(a + NZ)^2} (x_i - Z).$$

Hence, given \mathbf{z}_{t-1} , we approximate $\sum_{i=1}^N w(\mathbf{z}^{(i)}) / \sum_{i=0}^N w(\mathbf{z}^{(i)})$ by

$$\frac{\sum_{i=1}^N w(\mathbf{z}^{(i)})}{\sum_{i=0}^N w(\mathbf{z}^{(i)})} \approx \frac{NZ}{w(\mathbf{z}_{t-1}) + NZ} + \sum_{i=1}^N \frac{w(\mathbf{z}_{t-1})}{(w(\mathbf{z}_{t-1}) + NZ)^2} (w(\mathbf{z}^{(i)}) - Z) \quad (59)$$

$$= \frac{N^2 Z^2 + w(\mathbf{z}_{t-1}) \sum_{i=1}^N w(\mathbf{z}^{(i)})}{(w(\mathbf{z}_{t-1}) + NZ)^2} \quad (60)$$

so that

$$\mathbb{V}_{q_\lambda}[f | \mathbf{z}_{t-1}] \approx \mathbb{V}_{q_\lambda} \left[\frac{N^2 Z^2}{(w(\mathbf{z}_{t-1}) + NZ)^2} f_{IS} + \frac{w(\mathbf{z}_{t-1})}{(w(\mathbf{z}_{t-1}) + NZ)^2} \sum_{i=1}^N w(\mathbf{z}^{(i)}) f(\mathbf{z}^{(i)}) \right. \quad (61)$$

$$\left. + \frac{w(\mathbf{z}_{t-1})}{\sum_{i=0}^N w(\mathbf{z}^{(i)})} f(\mathbf{z}_{t-1}) \middle| \mathbf{z}_{t-1} \right]. \quad (62)$$

Observe that $\sum_{i=1}^N w(\mathbf{z}^{(i)}) f(\mathbf{z}^{(i)}) = O(N)$ since $\{\mathbf{z}^{(1)}, \dots, \mathbf{z}^{(N)}\}$ are independent and identically distributed and that $w(\mathbf{z}_{t-1}) f(\mathbf{z}_{t-1}) / \sum_{i=0}^N w(\mathbf{z}^{(i)}) = o(N)$. Combining these, we obtain

$$\mathbb{V}_{q_\lambda}[f | \mathbf{z}_{t-1}, \mathbf{z}^{(1:N)}] \approx \frac{N^4 Z^4}{(w(\mathbf{z}_{t-1}) + NZ)^4} \mathbb{V}_{q_\lambda}[f_{IS} | \mathbf{z}_{t-1}], \quad (63)$$

as was to be shown. \square